Biointerface Research in Applied Chemistry
Platinum Open Access Journal (ISSN: 2069-5837)

Article
Volume 11, Issue 6, 2021, 14986 - 14997
https://doi.org/10.33263/BRIAC116.1498614997

Removal and Comparative Adsorption of Anionic Dye on Various MgAl synthetic Clay

Ahmed Zaghloul [1,*], Abdeljalil Ait Ichou [1], M'hamed Abali [1], Ridouan Benhiti [1], Amina Soudani [2], Gabriela Carja [3], Mohamed Chiban [1], Mohamed Zerbet [1], Fouad Sinan[1,*]

1 Laboratory LACAPE, Faculty of Science, University Ibn Zohr, BP. 8106, Hay Dakhla, Agadir, Morocco
2 Faculty of Applied Sciences, University Campus Ait Melloul, Morocco
3 Laboratory of Materials Nanoarchitectonics, Faculty of Chemical engineering and Environment protection, Technical University of 'Gheorghe Asachi' of Iasi, Romania
* Correspondence: f.sinan@uiz.ac.ma (F.S.); zaghloul2013ahmed@gmail.com (A.Z.);

Scopus Author ID 55999934200

Received: 28.02.2021; Revised: 27.03.2021; Accepted: 29.03.2021; Published: 7.04.2021

Abstract: In this study, the adsorption of Congo red dye in an aqueous solution on two synthetic clay adsorbents, MgAl-LDH (2:1) and MgAl-LDH (3:1), was investigated using batch system experiments. The adsorbents' characterization was carried out by various techniques such as scanning electron microscopy (SEM), X-ray diffraction (XRD), and Fourier transform infrared spectroscopy FT-IR. The conditions applied in the adsorption experiments including the mass of adsorbent, initial concentration, contact time, pH, and temperature. The kinetic data were modeled by pseudo-first-order and pseudo-second-order. Langmuir and Freundlich's models analyzed the adsorption isotherms of Congo red on the two adsorbents. It was found that the adsorption process could be described by Langmuir isotherm. The maximum amount of adsorption is 285.71 and 166.66 mg/g for MgAl-LDH (2:1) and MgAl-LDH (3:1), respectively. Thermodynamic parameters such as enthalpy ΔH°, enthalpy ΔS°, and free enthalpy ΔG° were also evaluated to predict the nature of adsorption.

Keywords: layered double hydroxide; adsorption; Congo Red dye; wastewater treatment.

1. Introduction

For a long time, humankind tried to include dyes in many industries like textiles, stationery, cosmetics, and food. Due to their ease of synthesis and speed of production, synthetic dyes are the most widely used. In addition, the majority of these dyes are toxic and cause a lot of environmental and human health problems, hence the interest in treating wastewater from these industries [1]. Many treatment methods can be used for dye removal of wastewater; we can cite: adsorption [2,3], membrane filtration [4], chemical oxidation [5], ozonation [6], biological treatment [7], ion exchange [8], coagulation and flocculation [9].

Among these treatment methods, adsorption remains one of the most promising techniques because of its convenience and simplicity of use. In recent years, many researchers are increasingly interested in the use of adsorbents, which are both effective and low cost [10].

In recent years, layered double hydroxide (LDHs) have aroused great interest. Among the scientific community, these materials hold functional properties associated with specific structural properties, they can trap negatively charged species by surface adsorption or by anion exchange thanks to their positive surface charge and the flexibility of the interlayer space [11]. The present work investigates a practical and economical method for removing Congo red dye from water by adsorption on layered double hydroxide (LDHs) used as a novel synthetic adsorbent. Studies of certain parameters' influence have been carried out, such as the initial concentration of dye, mass of adsorbent, contact time, pH, and temperature. To better understand the dye's fixation mode, we were particularly interested in studying the kinetics, thermodynamics, and adsorption isotherms.

2. Materials and Methods

2.1. Preparation of LDHs and dye solution (CR).

The layered double hydroxides (LDHs) used in this work are produced by the urea method, with two deferent molar ratios (Mg^{2+}/Al^{3+} = 2 and 3), the experimental protocol for the synthesis of MgAl-LDH (2:1) and MgAl-LDH (3:1) by the urea method has been described by several authors [12,13].

The Congo Red (CR) solution that was used in this study was obtained by diluting a stock solution of dye with a mass concentration of $1 g.L^{-1}$. The stock pollutant solution was prepared by adding 1 gram of commercial dye powder to 1 liter of water (pH ≈ 6) in a volumetric flask. The physicochemical properties of Congo red (CR) are grouped together in Table 1.

Table 1. Some characteristics of Congo red dye.

Molecular structure	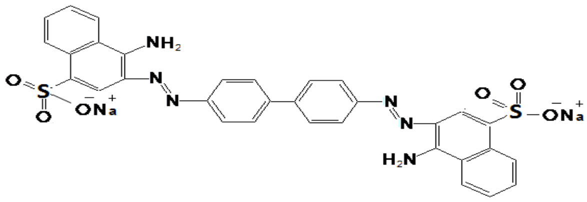
Molecular formula	$C_{32}H_{22}N_6Na_2O_6S_2$
Molar mass ($g. mol^{-1}$)	696.66
λ_{max} (nm)	497
Nature of charge	Anionic

2.2. Characterization of MgAl-LDH (2:1) and MgAl-LDH (3:1).

The crystal structure of MgAl-LDH (2:1) and MgAl-LDH (3:1) obtained was characterized using an X'PERT PRO MPD diffractometer with Cu/Kα radiation (45 kV, 40 mA) at 0.0670° step size. The morphology observations were carried out on a scanning electron microscope (SEM, UATRS CNRST). The FT-IR study was performed using FTIR 8400S, Shimadzu-FTIR spectra were recorded in the range 400-4000 cm^{-1} with the KBr pellet technique.

2.3. Adsorption procedure.

The adsorption tests were carried out in a batch reactor by stirring the colored synthetic solution of CR in the adsorbent's presence at a constant temperature. Homogenization of the mixtures was ensured by a magnetic bar stirrer with constant agitation. Samples were taken at regular time intervals after separation of the adsorbent adsorbate using a centrifuge at 3000 rpm for 15 minutes. The absorbance of the over-swimming solution was measured by a UV-visible spectrophotometer (JP Selecta SA, Barcelona, Spain) at the wavelength, which corresponds to the maximum absorbance of the CR (λ_{max} = 497 nm). The residual dye concentration is given by Beer Lambert's law from a calibration curve. The amount of the dye adsorbed at equilibrium is calculated by equation (1):

$$q_e = \left(\frac{C_0 - C_e}{m}\right) \times V \qquad (1)$$

With, V is the volume of solution (L), m is the mass of adsorbent (g), C_0 is the initial concentration of dye (mg/l), C_e is the equilibrium concentration of dye in the solution (mg/l), and q_e the amount of the dye adsorbed at equilibrium per unit mass of LDHs mg/g.

3. Results and Discussion

3.1. Characterization of MgAl-LDH (2:1) and MgAl-LDH (3:1).

The identification results of MgAl-LDH (2:1) and MgAl-LDH (3:1) were developed to indicate that the (XRD) lines of these materials (Fig.1) are typical to those of the structure of a published Mg and Al-based LDHs in the literature [12,14]. In general, the different XRD lines index in a compact hexagonal system with rhombohedral symmetry of symmetry group R-3m. The position of the first peak (003) allowed to calculate the cell parameter c ($c = 3d_{003}$), the line (110) located about 2θ = 60° is related to the cell parameter a such that $a = 2d_{110}$, this value corresponds to the metal-metal distance in the leaf. The calculated mesh parameters (a, c) and the interlamellar distance (d_{003}) for MgAl-LDH (2:1) and MgAl-LDH (3:1) are grouped together in Table 2.

The SEM (Fig. 2) examination shows that the adsorbents MgAl-LDH (2:1) and MgAl-LDH (3:1) are well synthesized under a hexagonal structure with good crystallinity [15,12].

The IR spectrum of two elaborate adsorbents shown in Figure 3 shows the main characteristic molecular groups for all layered double hydroxide phases [16]. The two bands located at 3341 cm^{-1} and 3395 cm^{-1} are attributed to the vibrations of the ν (OH) hydroxyl groups of the pseudo-brucite layer, including the water molecules intercalated and physically adsorbed [17]. In the middle of the spectrum, the intense band at 1632 cm^{-1} corresponds to the angular deformation vibration of the water molecules δ (H_2O) [18], The most intense adsorption peak at 1354 cm^{-1} is attributed to the vibration of carbonate ions [19]. The adsorption bands less than 800 cm^{-1} characterize the valence vibrations between oxygen and the metal ν (M-O), as well as the deformation vibrations of the oxygen-metal-oxygen leaves ν (M-O-M) [20,21].

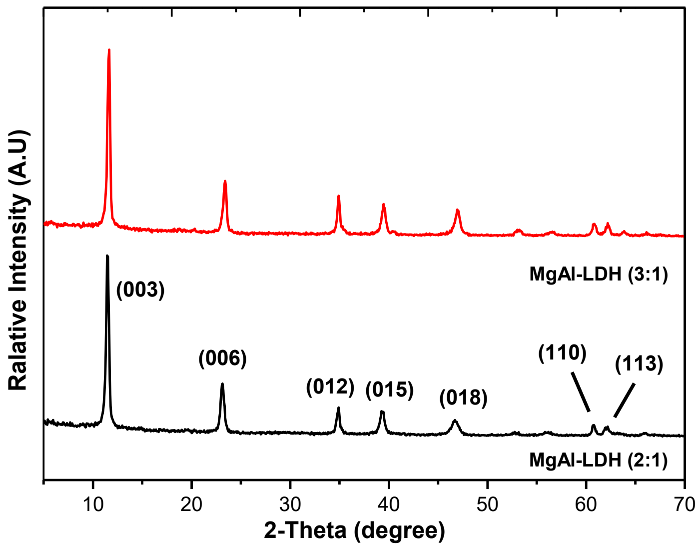

Figure 1. XRD patterns of LDHs.

Table 2. The values of cell parameters of MgAl-LDH (2:1) and MgAl-LDH (3:1).

adsorbent	d_{003} (Å)	d_{110} (Å)	a (A°)	c (Å)	λ (Å)
MgAl-LDH (2:1)	7,691	1,525	3,049	23,884	1.54
MgAl-LDH (3:1)	7,611	1,522	3,044	22,839	1.54

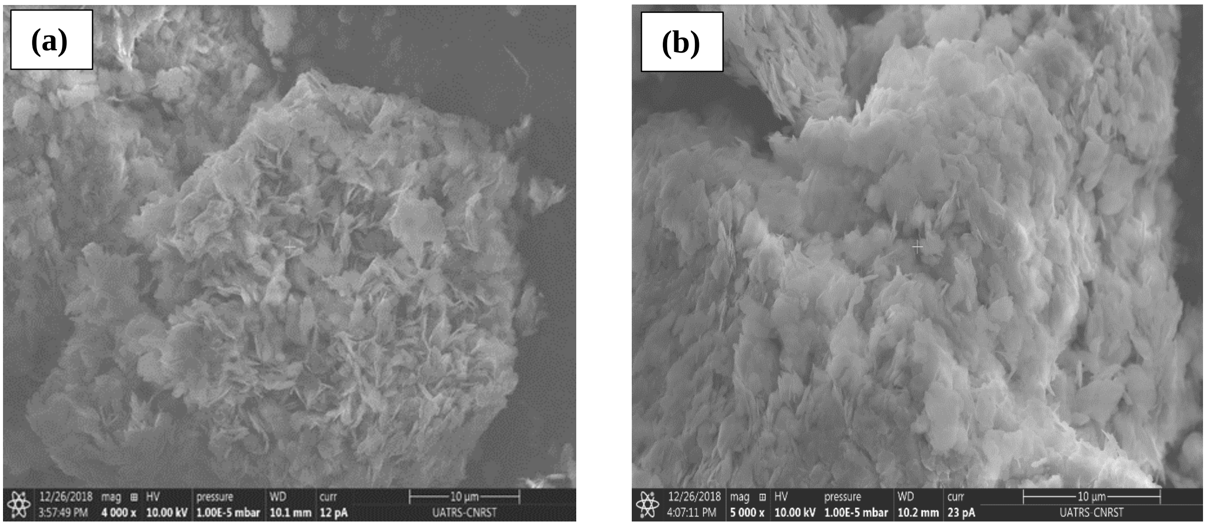

Figure 2. SEM images of the (**a**) MgAl-LDH (2:1); (**b**) MgAl-LDH (3:1).

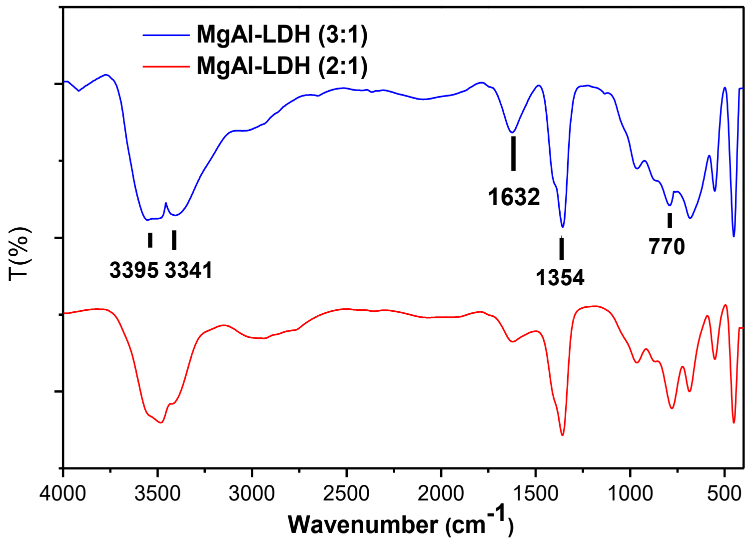

Figure 3. FTIR spectra of LDHs.

3.2. Adsorption of Congo red onto MgAl-LDH (2:1) and MgAl-LDH (3:1).

3.2.1. Effect of the adsorbent dosage.

Figure 4. Show the variation of the adsorbed quantity of Congo red on the sorbents MgAl-LDH (2:1) and MgAl-LDH (3:1) as a function of the mass. From this curve, it can be seen that the adsorbed amount increases with the increase in the amount of adsorbent suspended in the solution, then stabilize from a mass is equal to 20 mg. This result shows that 20 mg of LDHs per 40 ml of the dye solution is sufficient to reach maximum adsorption. For the rest of our study, the adsorption of Congo red on the two supports was carried out with mass = 20 mg.

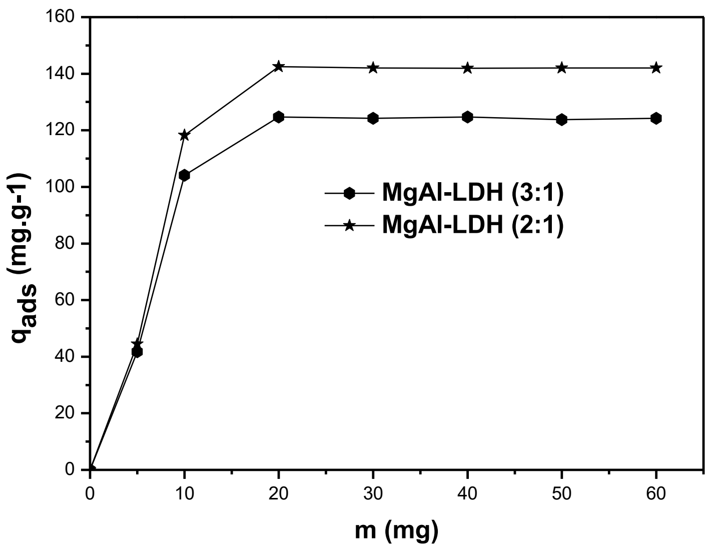

Figure 4. Effect of adsorbent dosage on the removal of CR by MgAl-LDH (2:1) and MgAl-LDH (3:1).

3.2.2. Effect of solution pH.

The pH of the environment is a parameter that positively or negatively affects the binding capacity of adsorbates [15]. Figure 5 shows the effect of the initial pH on the adsorbed amount of CR for the two adsorbents in a pH range of 2 to 12. In the pH range of 2 to pH = 8, for MgAl-LDH (2:1), and in pH 2 to 6 for and MgAl-LDH (3:1), the percentage of elimination is very important 74% and 62% for MgAl-LDH (2: 1), and MgAl-LDH (3:1) respectively, this is explained by strong electrostatic interactions between the solute (CR) and the positively charged H^+ surface of the adsorbent. For a value of pH = 8 for MgAl-LDH (2:1) and opH = 6 for MgAl-LDH (3:1), the adsorption decreases because of the competition between the excess OH^- in the solution and the anionic ions of CR.

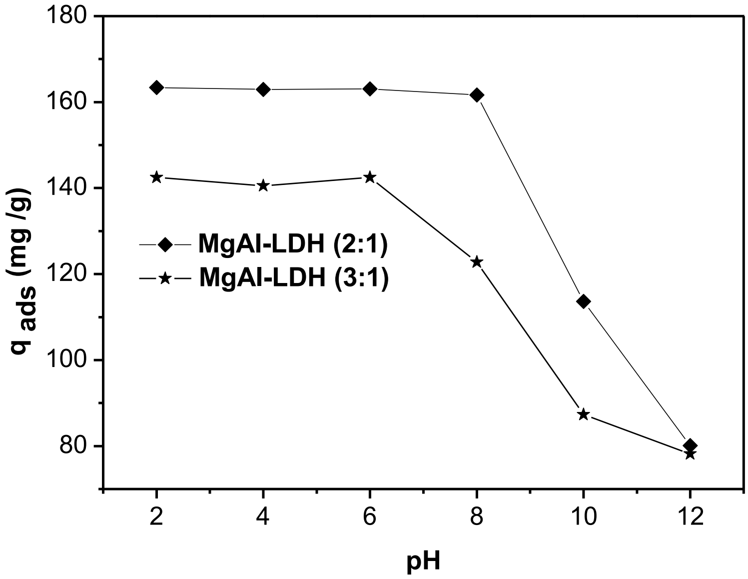

Figure 5. Effect of initial pH on the removal of CR.

3.2.3. Kinetic study of Congo red removal.

Figure 6 shows the effect of contact time on adsorption of CR by MgAl-LDH (2:1) and MgAl-LDH (3:1) at 100 $mg.L^{-1}$. Analysis of these curves reveals that the quantity adsorbed of Congo red by the two synthetic materials increases with the contact time. For two materials, MgAl-LDH (2:1) and MgAl-LDH (3:1), equilibrium was reached after 120 min. The adsorbed amount of two materials at equilibrium is 142.44 and 128.05 mg /g for MgAl-LDH (2:1) and MgAl-LDH (3:1), respectively. A similar study was carried out by A. Zaghloul *et al.* [15] on the adsorption of methyl orange by MgAl-LDH (2:1). They showed that the amount of MO fixed on the surface of this material increases as a function of time contact; they obtained equilibrium after 15 min with an adsorbed quantity of the order of 197 mg / g.

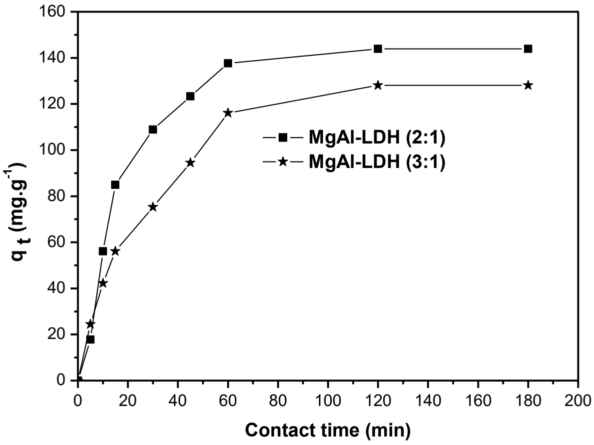

Figure 6. Effect of contact time on adsorption of Congo red.

The experimental data of the adsorption of CR on the two materials are tested by two kinetic models, the pseudo-first-order model (Eq.2), and the pseudo-second-order model (Eq.3).

$$\ln(q_e - q_t) = \ln q_e - k_1 t \quad (2)$$

$$\frac{t}{q_t} = \frac{1}{K_2 q_e^2} + \frac{1}{q_e} t \quad (3)$$

q_e and q_t (mg. g^{-1}) are the amounts of dye adsorbed onto MgAl-LDH (2:1) and MgAl-LDH (3:1) at equilibrium and at various time t (min); K_1 is the constant of the pseudo-first-order adsorption process (min^{-1}), and k_2 is the constant of the pseudo-second-order model of adsorption (g. mg^{-1} min^{-1}).

From Table 3, we note that the correlation coefficient R^2 of the reaction pseudo-second-order and pseudo-first-order is very important and that the values of the adsorption capacity q_e obtained from the two models are in agreement with the experimental values, which also confirms that the two models are the best to describe the adsorption kinetics of CR onto MgAl-LDH (2:1) and MgAl-LDH (3:1).

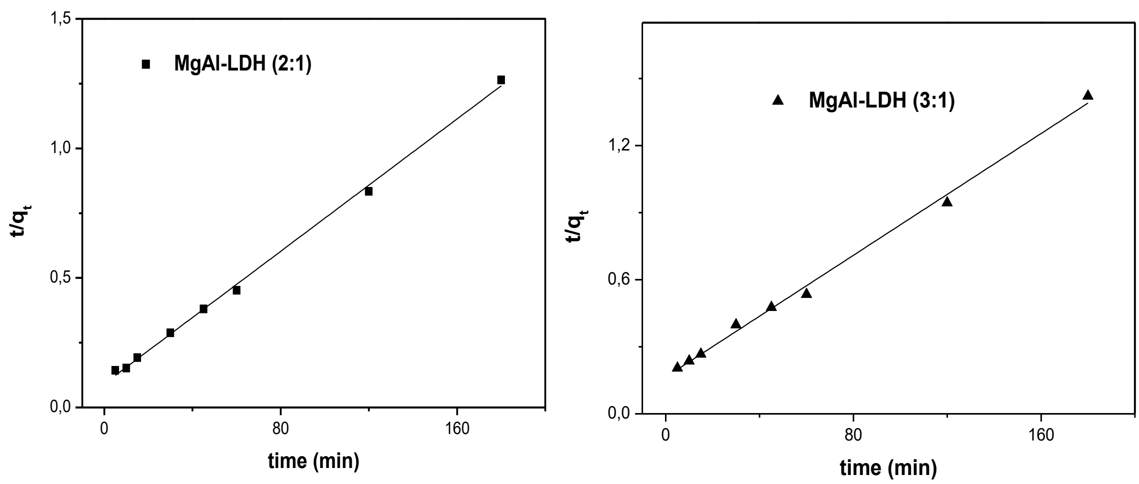

Figure 7. Pseudo-second-order kinetic model for the CR adsorption.

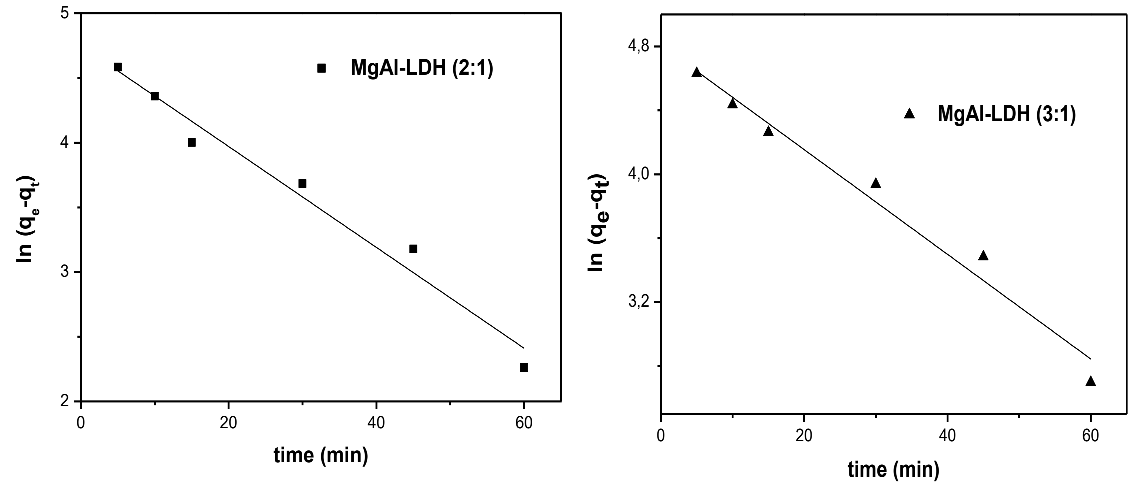

Figure 8. Pseudo-first-order kinetic model for the CR adsorption.

Table 3. Parameters of pseudo-first-order and pseudo-second-order kinetic models for the adsorption of CR on MgAl-LDH (2:1) and MgAl-LDH (3:1).

	q_e (exp) ($mg.g^{-1}$)	Pseudo-second-order			Pseudo-first-order		
		q_e ($mg.g^{-1}$)	K_2 ($g{\cdot}mg^{-1}.\ min^{-1}$)	R^2	q_e ($mg.g^{-1}$)	K_1 (min^{-1})	R^2
MgAl-LDH (2:1)	142.44	158.73	0.0004	0.99	193.35	0.05	0.98
MgAl-LDH (3:1)	128.05	149.25	0.0003	0.99	82.78	0.038	0.99

3.2.4. Effect of the initial concentration of dye.

To study the effect of this dye (CR) concentration on the two adsorbents, we have plotted the adsorbed quantity variation as a function of C_i, ranging from 50 to 400 mg/l (Figure 9). The results obtained show that the adsorbed amount of CR on the two adsorbents increases with increasing initial concentration. This can be explained by increasing the dye transfer rate at a higher initial concentration, which subsequently causes the adsorption of several dye molecules [22]. It should then be noted that the quantity adsorbed stabilizes when the supports are saturated. D. Bharali *et al.* [23] reported a similar study on eliminating CR by LDHs using adsorbent NiAl-LDH.

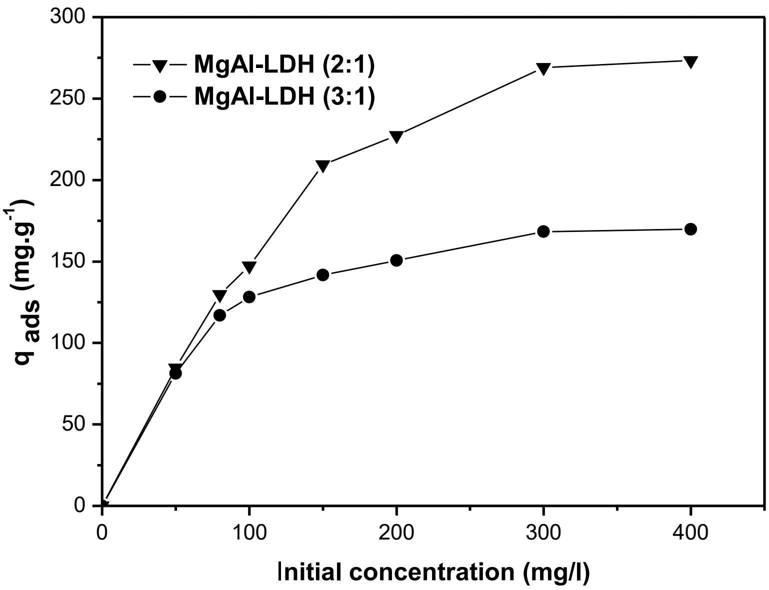

Figure 9. Effect of initial concentration of Congo Red.

3.3. Isotherms adsorption.

The adsorption isotherms of CR on MgAl-LDH (2:1) and MgAl-LDH (3:1) are performed under the optimum conditions mentioned above for the initial concentration effect. Figures 10 and 11 present the plots of the formalisms of Langmuir $1/q_e = f(1/Ce)$ Eq (4) and of Freundlich $Lnq_e = f(Ln\ C_e)$ Eq (5).

$$\frac{1}{q_e} = \frac{1}{q_m K_L}\frac{1}{C_e} + \frac{1}{q_m} \qquad (4)$$

With q_m: Capacity maximum adsorbed (mg/g), K_L: adsorbent characteristic equilibrium constant ($L.mg^{-1}$), dependent on temperature and experimental conditions, C_e: adsorbate concentration at equilibrium ($mg.L^{-1}$).

$$Lnq_e = 1/n\ LnC_e + Ln\ K_F \qquad (5)$$

K_F and 1/n are Freundlich's constants characteristic of the efficiency of a given adsorbent to a given solute. The values of the correlation coefficients and the various equilibrium parameters are grouped in Table 4.

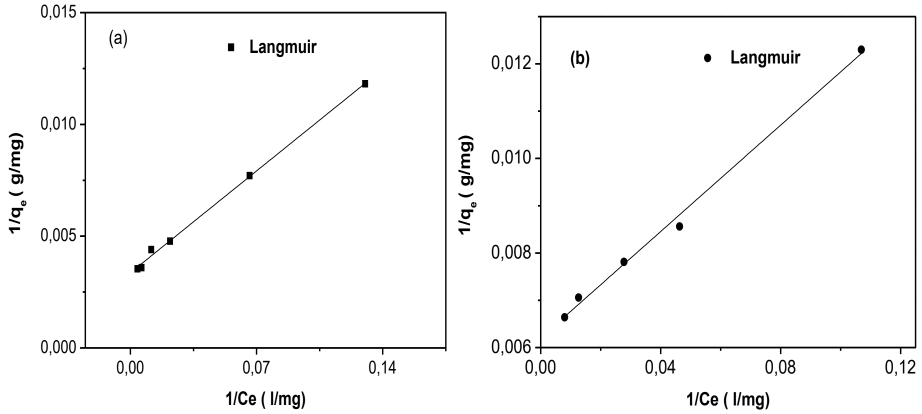

Figure 10. Langmuir adsorption isotherm for adsorption of CR, **(a)** MgAl-LDH (2:1); **(b)** MgAl-LDH (3:1).

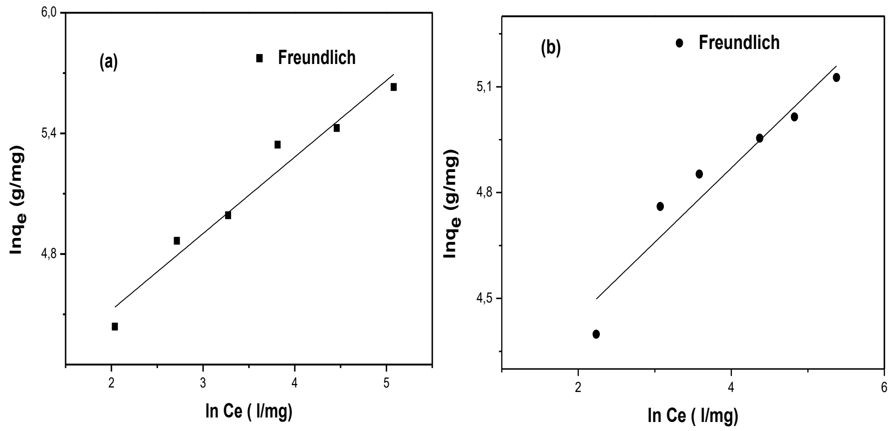

Figure 11. Freundlich adsorption isotherm for adsorption of CR, **(a)** MgAl-LDH (2:1); **(b)** MgAl-LDH (3:1).

Table 4. Parameters of Langmuir and Freundlich isotherm models for adsorption of CR on MgAl-LDH (2:1) and MgAl-LDH (3:1) adsorbents.

Langmuir				Freundlich		
Adsorbent	q_m ($mg.g^{-1}$)	K_L ($L.mg^{-1}$)	R^2	K_F ($mg.g^{-1}$)	1/n	R^2
MgAl-LDH (2:1)	285.71	0.05	0.99	48.53	0.34	0.95
MgAl-LDH (3:1)	166.66	0.10	0.99	75.83	0.14	0.92

From an observation window of these results, the Langmuir isotherm appears to be the most satisfactory for the adsorption modeling of the CR on the two materials prepared with good correlations (R^2 = 0.99) for MgAl-LDH (2:1) and MgAl-LDH (3:1) respectively.

Therefore, the adsorption of CR on the two adsorbents is monolayer, resulting in adsorption on independent sites of the same nature. The maximum adsorption capacities q_m of the RC calculated using the Langmuir model are very important 285.71 and 166.66 mg / g for the material MgAl-LDH (2:1) and MgAl-LDH (3:1), respectively. The values of 1/n calculated from the Freundlich isotherm are always less than unity, this shows that the adsorption of Congo red on the two prepared LDHs is favorable. D. Bharali *et al.* [23] showed in their study of the adsorption of CR on Ni and Al-based LDHs that the adsorption is best described by the Langmuir isotherm, which indicates the homogeneous nature of the surfaces of the samples and forming a monolayer of CR molecules on the surface of the adsorbent.

3.4. Thermodynamic studies.

Thermodynamic parameters such as standard free enthalpy ΔG°, standard enthalpy ΔH°, and standard entropy ΔS° were determined using the following equations [24].

$$K_d = \frac{q_e}{C_e} \quad (6)$$

$$\Delta G° = -RT Ln K_d \quad (7)$$

$$Ln K_d = \frac{\Delta S°}{R} - \frac{\Delta H°}{RT} \quad (8)$$

The values of enthalpy and entropy were obtained from the linear plot of the variation of LnK_d as a function of 1/ T (Fig. 12); ΔH° / R and ΔS°/ R are the slope and the y-intercept, respectively. From these results (Table 5), we find that the negative values of adsorption ΔG° of the RC on the two adsorbents imply that the adsorption process was spontaneous [25]. The values of ΔG° shows that it is physisorption (ΔG° between -20 and 0 kJ / mole) we also note that ΔG° increases with the increase in the temperature of the solution for the two supports studied, which can be explained by the fact that adsorption becomes very difficult and disadvantaged when the temperature becomes very high [26]. The calculated enthalpy values at different temperatures are less than zero (ΔH°< 0), which shows that this process is exothermic for both materials. The negative ΔS° value for the two adsorbents shows that the adsorption takes place with increasing order at the solid-solution interface [27].

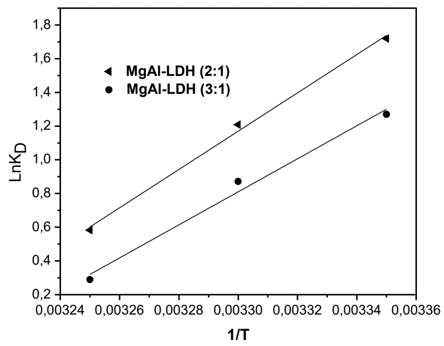

Figure 12. Linear plots of LnK_D vs. 1/T for the determination of thermodynamic parameters.

Table 5. Thermodynamic adsorption parameters of CR and on the two materials.

Adsorbent	T (k)	K_D	ΔG° ($kJ.mol^{-1}$)	ΔS° ($J.mol^{-1}.K^{-1}$)	ΔH° ($Kj.mol^{-1}$)
MgAl-LDH (2:1)	298.15	5,58	-4,26	-227.58	-72.14
	303.15	3,56	-3,14		
	308.15	2,17	-1,92		
MgAl-LDH (3:1)	298.15	3,56	-3,14	-239.98	-74.77
	303.15	2,38	-2,15		
	308.15	1,33	-0,71		

3.5. Comparison with other adsorbents.

The maximum removal efficiency of CR with some materials in the literature is mentioned in Table 6. Comparing the adsorption values of CR, we notice that the two materials prepared have very interesting adsorption properties.

Table 6. Maximum adsorption capacities (mg/g) of CR on the different adsorbents.

Adsorbent	$C_{initiale}$ (mg/L)	q_{max} (mg.g^{-1}	Reference
NiAl-S_1 LDH	10	120.5	[23]
MgAl-LDH	20	111.1	[28]
NiO/GO nanosheets	20	123.89	[29]
Activated red mud	10	7.08	[30]
Coir pith activated carbon	20	6.72	[31]
Fe_3O_4@graphene	10	33.66	[32]
AgNPs-coated AC	20	64.80	[33]
AuNPs-coated AC	20	71.05	[33]
3D hierarchical GO-NiFe LDH	-	489	[34]
MgAl-LDH (2:1)	50-400	285.71	This study
MgAl-LDH (3:1)	50-400	166.66	This study

4. Conclusions

The preparation of layered double hydroxide MgAl with two molar ratios $M^{2+}/M^{3+} = 2$ and 3, was carried out by the urea method. The study of the absorption process of Congo Red on MgAl was the subject of this work. The result of XRD and FTIR characterization shows that the two materials used are typical of those of the structure of LDHs published in the literature, the results obtained relating to the kinetics, thermodynamics, and adsorption isotherms were exploited to clarify the mode of attachment of the dye to the adsorbent. The study of the influence of time effect on kinetics has shown that the adsorption process follows both pseudo-second-order and first-order patterns. Langmuir's model best expresses the type of adsorption; the dye molecules are then adsorbed in monolayers without any dye-dye interactions, which increases the order of their distribution on the adsorbent surface. The three thermodynamic parameters' negative values characterized the reaction as exothermic and spontaneous physisorption, during which the order of distribution of the dye molecules on the potato peels increases relative to that in solution. In addition, the increase in $\Delta G°$ values with increasing temperature has proven that the feasibility of adsorption decreases at elevated temperatures. All of these results reveal that the two materials MgAl-LDH (2:1) and MgAl-LDH (3:1) could be used effectively as a low-cost adsorbent for the removal of the Congo red dye from an aqueous solution.

Funding

This research received no external funding.

Acknowledgments

This research has no acknowledgment.

Conflicts of Interest

The present paper is an original work, and all the authors declare that they have no conflicts of interest.

References

1. Zaghloul, A.; Benhiti, R.; Abali, M.; Ait Ichou, A.; Soudani, A.; Chiban, M.; Zerbet, M.; Sinan, F. Kinetic, isotherm, and thermodynamic studies of the removal of methyl orange by synthetic clays prepared using urea or coprecipitation. *EuroMediterr J Environ Integr* **2021**, *6*, 2-10, https://doi.org/10.1007/s41207-020-00217-4.
2. Alhaji, N.M.I.; Nathiya, D.; Kaviyarasu ,K.; Meshram ,M.; Ayeshamariam, A. A comparative study of structural and photocatalytic mechanism of $AgGaO_2$ nanocomposites for equilibrium and kinetics evaluation of adsorption parameters. *Surf. Interfaces* **2019**, *17*, 100375, https://doi.org/10.1016/j.surfin.2019.100375.
3. Shabaan, OA .; Jahin, H S.; Mohamed, GG. Removal of anionic and cationic dyes from wastewater by adsorption using multiwall carbon nanotubes. *Arab. J. Chem* **2020**, *13*, 4797-4810, https://doi.org/10.1016/j.arabjc.2020.01.010.
4. Mansor, ES.; Alib, H .; Abdel-Karim, A . Efficient and reusable polyethylene oxide/polyaniline composite membrane for dye adsorption and filtration. *Colloids Interface Sci. Commun* **2020,** *39*, 100314, https://doi.org/10.1016/j.colcom.2020.100314.
5. Medrano-Rodríguez, F.; Picos-Benítez, A.; Brillas, E.; Bandala, ER.; Pérez, T.; and Peralta-Hernández, JM. Décoloration par oxydation électrochimique avancée et élimination de trois colorants bruns diazo utilisés dans l'industrie de la tannerie. *J. Electroanal. Chem* **2020**, *873*, 114360, https://doi.org/10.1016/j.jelechem.2020.114360.
6. Turhan, K.; Turgut, Z. Decolorization of direct dye in textile wastewater by ozonization in a semi-batch bubble column reactor. *Desalination* **2009**, *242*, 256–263, https://doi.org/10.1016/j.desal.2008.05.005.
7. Mojtabavi, S.; Khoshayand, MR.; Fazeli, MR.; Samadi, N.; Faramarzi, MA. Combinaison de traitements thermiques et biologiques pour la bio-élimination et la détoxification de certains colorants synthétiques récalcitrants par la laccase thermostabilisée induite par la bétaïne. *Environ. Technol. Innov* **2020**, *20*, 101046, https://doi.org/10.1016/j.eti.2020.101046.
8. Joseph, J.; Radhakrishnan, R. C.; Johnson, J.K .; Joy, S.P.; Thomas, J. Ion-exchange mediated removal of cationic dye-stuffs from water using ammonium phosphomolybdate. *Mater. Chem. Phys* **2020**, *242*, 122488, https://doi.org/10.1016/j.matchemphys.2019.122488.
9. Beluci, N.C.L.; Mateus, G.A.P.; Miyashiro, C.S.; Homem, N.C.; Gomes, R.G.; Fagundes-Klen, M.R.; Bergamasco, R.; Vieira, A.M. Hybrid treatment of coagulation/flocculation process followed by ultrafiltration in TIO_2-modified membranes to improve the removal of reactive black 5 dye. *Sci. Total Environ* **2019,** *664*, 222–229, https://doi.org/10.1016/j.scitotenv.2019.01.199.
10. Anastopoulos, I.; Margiotoudis, I.; Massas, I. The use of olive tree pruning waste compost to sequestrate methylene blue dye from aqueous solution. *Int.J. Phytoremediat* **2018**, *20*, 831-838, https://doi.org/10.1080/15226514.2018.1438353.
11. Theiss, F.L.; Couperthwaite, S.J.; Ayoko, G.A.; Frost, R.L. A review of the removal of anions and oxyanions of the halogen elements from aqueous solution by layered double hydroxides. *J Colloid Interf Sci* **2014**, *417*, 356–368, https://doi.org/10.1016/j.jcis.2013.11.040.
12. Zaghloul, A.; Ait Ichou, A.; Benhiti, R.; Abali, M.; Soudani, A.; Chiban, M.; Zerbet, M.; and Sinan, F. Removal of methyl orange from aqueous solution using synthetic clay type MgAl-LDH: Characterization, Isotherm and thermodynamic studies. *Mediterr. J. Chem* **2019**, *9* 155-163, http://dx.doi.org/10.13171/mjc92190925728fs.
13. Benhiti, R.; Ait Ichou, A.; Zaghloul, A.; Aziam, R .; Carja, G.; Zerbet, M.; Sinan, F.; Chiban, M. Synthesis, characterization, and comparative study of MgAl-LDHs prepared by standard coprecipitation and urea hydrolysis methods for phosphate removal. *Environ Sci Pollut Res* **2020**, *27*, 45767-45774, https://doi.org/10.1007/s11356-020-10444-5.
14. Ait Ichou, A.; Benhiti, R.; Abali, M.; Dabagh, A.; Chiban, M.; Zerbet, M.; Carja, G.; Sinan, F. Adsorption of Pb(II) from aqueous solutions onto MgFeAl-CO_3 LDH: thermodynamic and kinetic studies. *DESALIN WATER TREAT* **2020**, *178*, 193–202, https://doi.org/10.5004/dwt.2020.24952.
15. Zaghloul, A.; Benhiti, R.; Ait Ichou, A.; Carja, G.; Soudani, A.; Zerbet, M.; Sinan, F.; Chiban, M. Characterization and application of MgAl layered double hydroxide for methyl orange removal from aqueous solution. *Materials Today: Proceedings* **2021**, *37*, 3793-3797, https://doi.org/10.1016/j.matpr.2020.07.676.
16. Xie, J.; Yamaguchi, T.; Oh, J-M. Synthesis of a mesoporous Mg–Al–mixed metal oxide with P123 template for effective removal of Congo red via aggregation-driven adsorption. *J. Solid State Chem* **2021**, *293*, 121758, https://doi.org/10.1016/j.jssc.2020.121758.

17. Deák, A.; Csapó, E.; Juhász, A.; Dékány, I.; Janovák, L. Anti-ulcerant kynurenic acid molecules intercalated Mg/Al-layered double hydroxide and its release study. *Appl. Clay Sci* **2018**, *156*, 28–35, https://doi.org/10.1016/j.clay.2018.01.024.
18. Benhiti, R.; Ait Ichou, A.; Zaghloul, A.; Carja, G.; Zerbet, M.; Sinan, F.; Chiban, M. Kinetic, isotherm, thermodynamic and mechanism investigations of dihydrogen phosphate removal by MgAl-LDH. *Nanotechnol. Environ. Eng.* **2021**, 6, 16. https://doi.org/10.1007/s41204-021-00110-7.
19. Zhang, W.; Liang, Y.; Wang, J.; Zhang, Y.; Gao, Z.; Yang, Y.; Yang, K. Ultrasound-assisted adsorption of Congo red from aqueous solution using $MgeAleCO_3$ layered double hydroxide. *Appl. Clay Sci* **2019**, *174*, 100–109, https://doi.org/10.1016/j.clay.2019.03.025.
20. Dooraid, N.A.; Naji, L.A.; Faisal, A.H.; Al-Ansari, N.; Naushad, M. Waste foundry sand/MgFe-layered double hydroxides composite material for efficient removal of Congo red dye from aqueous solution. *Scientific Reports* **2020**, *10*, 2042, https://doi.org/10.1038/s41598-020-58866-y.
21. Sriram, G.; Uthappa, U. T.; Losic, D .; Kigga, M .; Jung, Ho.Y.; and. Kurkuri, M.D. Mg–Al-Layered Double Hydroxide (LDH) Modified Diatoms for Highly Efficient Removal of Congo Red from Aqueous Solution. *Appl. Sci*. **2020**, *10*, 2285, https://doi.org/10.3390/app10072285.
22. Bouberka, Z.; Kacha, S.; Kameche, M.; Elmaleh, S.; Derriche, Z. Sorption study of an acid dye from an aqueous solutions using modified clays. *J. Hazard. Mater* **2005**, *119*, 117-124, https://doi.org/10.1016/j.jhazmat.2004.11.026.
23. Bharali, D.; Deka, R. Adsorptive Removal of Congo Red from aqueous Solution by Sonochemically Synthesized NiAl Layered Double Hydroxide. *Environ. Chem. Eng* **2017**, 2056-2067, https://doi.org/10.1016/j.jece.2017.04.012.
24. Zubair, M.; Jarrah, N.; Ihsanullah; Khalid, A.; Manzar, M.; Kazeem, T.; Al-Harthi, M.A. Starch-NiFe-layered double hydroxide composites: Efficient removal of methyl orange from aqueous phase. *J MOL LIQ* **2018**, *249*, 254–264, https://doi.org/10.1016/j.molliq.2017.11.022.
25. Güzel, F.; Sayğılı, H.; Sayğılı, G.A.; Koyuncu F. Decolorisation of aqueous crystal violet solution by a new nanoporous carbon: Equilibrium and kinetic approach. *J. Ind. Eng. Chem* **2014**, *20*, 3375-3386, https://doi.org/10.1016/J.JIEC.2013.12.023.
26. Meçabih, Z.; Kacimi, S.; Bouchikhi, B. Adsorption of organic matter, from urban wastewater, onto bentonite modified by Fe(III), Al(III and Cu(II). *Rev. Des Sci. De L'Eau* **2006**, *19*, 23-31, https://doi.org/10.7202/012261ar.
27. Aarfane, A.; Salhi, A, El Krati, M.; Tahiri, S.; Monkade, M.; Lhadi, E.K.; Bensitel, M. Kinetic and thermodynamic study of the adsorption of Red195 and Methylene blue dyes on fly ash and bottom ash in aqueous medium. *J. Mater. Environ. Sci* **2014**, *5*, 1927-1939.
28. Lafi, R.; Charradi, K.; Djebbi, M.A.; Amara, A.B.H.; Hafiane, A. Adsorption study of Congo red dye from aqueous solution to Mg-Al-layered double hydroxide. *J. Adv. Powder Technol* **2016**, *27*, 232–237, https://doi.org/10.1016/j.apt.2015.12.004.
29. Rong, X.; Qiu, F.; Qin, J.; Zhao, H.; Yan, J.; Yang, D. A facile hydrothermal synthesis, adsorption kinetics and isotherms to Congo Red azo-dye from aqueous solution of NiO/graphene nanosheets adsorbent. *J. Ind. Eng. Chem* **2015**, *26*, 354–363, https://doi.org/10.1016/j.jiec.2014.12.009.
30. Tor, A.; Cengeloglu, Y. Removal of Congo red from aqueous solution by adsorption onto acid activated red mud. *J. Hazard. Mater* **2006**, *138*, 409 – 415, https://doi.org/10.1016/j.jhazmat.2006.04.063.
31. Namasivayam, C.; Kavitha, D. Removal of Congo Red from Water by Adsorption onto Activated Carbon Prepared from Coir Pith, an Agricultural Solid Waste. *J. Dyes Pigm* **2002**, *54*, 47–58, https://doi.org/10.1016/S0143-7208(02)00025-6.
32. Yao ,Y.; Miao, S.; Liu, S.; Ma, L.P.; Sun ,H.; Wang S . Synthesis, characterization, and adsorption properties of magnetic Fe3O4@graphene nanocomposite. *Chem. Eng J* **2012**, *184*, 326–332, https://doi.org/10.1016/j.cej.2011.12.017.
33. Pal, J.; Deb, M.K. Efficient adsorption of Congo red dye from aqueous solution using green synthesized coinage nanoparticles coated activated carbon beads. *J. Appl. Nano Sci* **2014**, *4*, 967–978, https://doi.org/10.1007/s13204-013-0277-y.
34. Zheng, Y.; Cheng, B .; You, W.; J, Yu .; W, Ho. 3D hierarchical graphene oxide-NiFe LDH composite with enhanced adsorption affinity to Congo red, methyl orange and Cr(VI) ions. *J. Hazard. Mater* **2019**, *369*, 214–225, https://doi.org/10.1016/j.jhazmat.2019.02.013.